

# Particle production in high-energy collisions beyond the shockwave limit

Tolga Altinoluk<sup>a</sup> and Adrian Dumitru<sup>b,c</sup>

<sup>a</sup> Departamento de Física de Partículas and IGFAE,

Universidade de Santiago de Compostela, E-15706 Santiago de Compostela, Galicia-Spain

<sup>b</sup> Department of Natural Sciences, Baruch College,

CUNY, 17 Lexington Avenue, New York, NY 10010, USA

<sup>c</sup> The Graduate School and University Center, The City University of New York,  
365 Fifth Avenue, New York, NY 10016, USA

We compute next to eikonal (NE) and next to next to eikonal (NNE) corrections to the Lipatov vertex due to a finite target thickness. These arise from electric field insertions into the eikonal Wilson lines and give rise to corrections to gluon production proportional to the thickness of the target,  $A^{1/3}$ . We then derive a  $k_T$ -factorization formula for single inclusive gluon production at NNE accuracy. We also analyze NNE corrections on two-gluon production.

Production of particles with moderately high transverse momentum in high-energy hadronic collisions probes the gluon fields of the projectile or target at small light-cone momentum fractions [1]. The field (in light-cone gauge,  $A^+ = 0$ ) in the forward light cone of a collision of two infinitely thin charge sheets (shock waves) is given by [2–4]

$$p^2 A^{i,a}(p) = (T^a)_{bc} g^3 \int dz_1^- dz_2^+ \int \frac{d^2 k}{(2\pi)^2} L^i(p, k) \frac{\rho_1^b(z_1^-, k) \rho_2^c(z_2^+, p - k)}{k^2 (p - k)^2}. \quad (1)$$

Here  $p$  is the transverse momentum of the produced gluon and  $L^i(p, k)$  is the Lipatov vertex [5],

$$L_i(p, k) L_i^*(p, q) = \frac{4}{p^2} [\delta^{ij} \delta^{lm} + \epsilon^{ij} \epsilon^{lm}] k^i (p - k)^j q^l (p - q)^m. \quad (2)$$

In eq. (1)  $\rho_{1,2}$  denote the random color charge densities of projectile and target, respectively, which will be averaged over. The equation is valid to leading order in both color charge densities; a generalization to all orders in  $\rho_2$  was given in ref. [6].

Eq. (2) applies in the shockwave limit where the projectile charges propagate on eikonal trajectories through the field generated coherently by all valence charges in the target. Ref. [4], for example, offers a very clear discussion. However, at finite energies the non-zero thickness  $\ell^+$  of the target should be taken into account when  $p^2 \ell^+ / p^+ \sim p \ell^+ e^{-y}$  is not negligible. This is the case, in particular, for heavy-ion targets since  $\ell^+ \sim A^{1/3}$ . We should emphasize that our focus here is not on finite- $x$  corrections to the small- $x$  evolution of the unintegrated gluon distribution. Such evolution equations for some specific gluon distributions have been derived in ref. [7] to order  $(\ell^+ / p^+)^0$ . Furthermore, kinematic finite energy corrections not proportional to the target thickness have been derived by Babansky and Balitsky [8]; they find that such corrections are important for dipole-dipole scattering at rapidity  $\lesssim 5$ . Rather, here we consider corrections to the particle production vertex beyond the shockwave approximation for the *valence* charges; this is a nuclear effect proportional to  $A^{1/3}$  and should be relevant in particular for a heavy-ion target.

The gluon production cross section then involves one or more electric field insertions into the eikonal Wilson lines [9, 10], i.e. operators such as

$$\mathcal{U}_{[0,1]}^{i,ab}(x^+, y^+, y_\perp) = \int_{y^+}^{x^+} dz^+ \frac{z^+ - y^+}{x^+ - y^+} \mathcal{U}^{ac}(x^+, z^+, y_\perp) [ig T_{cd}^e \partial_{y^i} A^{-,e}(z^+, y_\perp)] \mathcal{U}^{db}(z^+, y^+, y_\perp), \quad (3)$$

where

$$\mathcal{U}(x^+, y^+, y_\perp) = \mathcal{P} e^{ig \int_{y^+}^{x^+} dz^+ T \cdot A^-(z^+, y_\perp)} \quad (4)$$

are the usual eikonal lines. Note that besides the electric field insertion which is due to the finite target thickness the Wilson line (3) does run along the light cone. For a study of kinematic corrections corresponding to Wilson lines at a finite angle (rapidity) we refer to ref. [8].

The new Wilson lines with electric field insertions appear due to quantum diffusion of the incident projectile in the transverse direction as it passes through a target of finite thickness  $\ell^+$ . At leading order in the field of the target the

above Wilson line simplifies to

$$\mathcal{U}_{[0,1]}^{i,ab}(x^+, y^+, y_\perp) = \int_{y^+}^{x^+} dz^+ \frac{z^+ - y^+}{x^+ - y^+} [igT_{ab}^e \partial_{y^i} A^{-,e}(z^+, y_\perp)] \quad (5)$$

which suffices for the evaluation of the Lipatov vertex. The purpose of this paper is to derive  $L_i$  at next to next to eikonal (NNE) accuracy; and to discuss the corrections to the single-inclusive gluon production cross section at high transverse momentum at order  $\rho_T(k_1) \rho_T^*(k_2)$ .

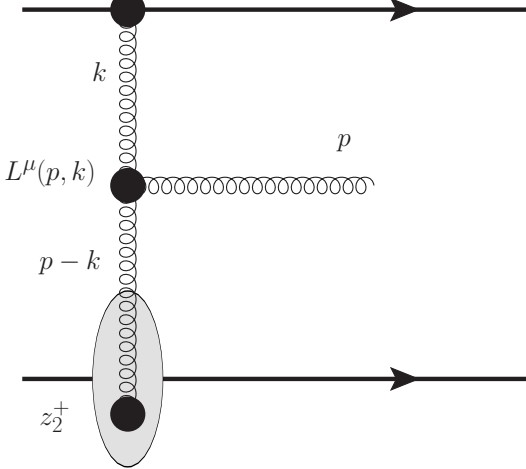


FIG. 1: Fusion of the fields of two high-energy projectile and target charges described by the Lipatov vertex.

Our result for the Lipatov vertex (in light-cone gauge  $A^+ = 0$ ) at NNE accuracy is

$$L^i(p, k) = -2C^i(p, k) k^2 \left\{ 1 + \frac{i}{2} p^2 \frac{z_2^+}{p^+} - \frac{1}{8} \left( p^2 \frac{z_2^+}{p^+} \right)^2 \right\}, \quad (6)$$

where

$$C^i(p, k) = \frac{p^i}{p^2} - \frac{k^i}{k^2}. \quad (7)$$

A derivation is given in appendix A and the corresponding diagram is shown in fig. 1. The first term in (6) corresponds to the eikonal (shock wave) limit while the second and third terms are the NE and NNE corrections for a target of finite thickness  $\ell^+$ , respectively. These corrections come with additional factors of  $z_2^+/p^+$  which is due to the above mentioned quantum diffusion of the incident wave passing through the target. The mean square deviation from the classical (eikonal) path is proportional to  $z_2^+/p^+$  [10].

The vertex from eq. (6) acts on a product of projectile and target fields to generate the produced gluon radiation field in the forward light cone,

$$\mathcal{M}_\lambda^a(p) = \epsilon_\lambda^i p^2 A^{i,a}(p), \quad (8)$$

with  $p^2 A^{i,a}(p)$  as written in eq. (1) above.

To compute the single inclusive cross section we multiply eq. (8) with its complex conjugate, sum over gluon polarizations and colors, and perform an average over the random color charge densities of projectile and target. In the standard McLerran-Venugopalan (MV) model [11] this (target) average is performed with the action

$$S_{\text{MV}}[\rho] = \int d^2 x_\perp dx^+ \frac{\text{tr} \rho(x^+, x_\perp) \rho(x^+, x_\perp)}{\mu^2}, \quad (9)$$

which leads to the following color charge correlator:

$$\langle \rho^a(z_1^+, k_1) \rho^{*b}(z_2^+, k_2) \rangle = \delta^{ab} \delta(z_1^+ - z_2^+) (2\pi)^2 \delta^2(k_1 - k_2) \mu^2. \quad (10)$$

$\mu^2$  denotes the mean color charge density (squared) per unit transverse area and longitudinal phase space. Because color charge correlations in the MV model are local in  $z^+$ , sub-eikonal corrections, i.e. the curly brackets in eq. (6), cancel[18] in the (absolute) square of the amplitude (8).

One may also consider a generalization of the MV-model action where the two color charge densities sit at different longitudinal coordinates,

$$S_{\text{eff}}[\rho] = \frac{1}{\ell^+} \int d^2x_\perp dx^+ dy^+ \frac{\text{tr } \rho(x^+, x_\perp) U_{x^+ \rightarrow y^+} \rho(y^+, x_\perp) U_{y^+ \rightarrow x^+}}{\mu^2}, \quad (11)$$

and are connected by gauge links along the longitudinal axis. At leading order in  $gA^-$  we then consider the color charge correlator

$$\langle \rho^a(z_1^+, k_1) \rho^{*b}(z_2^+, k_2) \rangle = \delta^{ab} \Theta(\ell^+ - |z_1^+ - z_2^+|) \frac{1}{\ell^+} (2\pi)^2 \delta^2(k_1 - k_2) \mu^2. \quad (12)$$

This correlator reduces to the MV-model one from eq. (10) in the limit  $\ell^+ \rightarrow 0$ .

In appendix B we show that eq. (12) leads to a single-inclusive cross section given by

$$p^+ \frac{d\sigma}{dp^+ d^2p d^2b} = 4N_c(N_c^2 - 1) S_\perp \frac{g^2}{p^2} \left[ 1 - \frac{1}{3} \left( \frac{p^2 \ell^+}{4p^+} \right)^2 \right] \int \frac{d^2k}{(2\pi)^2} \Phi_P(k^2) \Phi_T((p - k)^2). \quad (13)$$

Here,  $S_\perp$  denotes the transverse area of the collision. In eq. (13) we introduced the unintegrated gluon distribution of the target via

$$\Phi_T(k^2) = g^2 \ell^+ \frac{\mu_T^2}{k^2}, \quad (14)$$

and similar for the projectile. This function is dimensionless and proportional to the saturation momentum squared,  $Q_s^2 \sim g^4 \ell^+ \mu^2$ . However, saturation of the gluon density at low  $k^2$  is not incorporated in (14) which exhibits the perturbative  $\sim 1/k^2$  growth down to low transverse momentum.

We note that in eq. (13) NE corrections  $\sim p^2 \ell^+ / p^+$  drop out, see also refs. [9, 10] and appendix B. The NNE correction corresponds to the second term in the square brackets. As already indicated above it is suppressed by two powers of the light-cone momentum  $p^+$  of the produced gluon but exhibits nuclear enhancement  $\sim (\ell^+)^2$  with  $\ell^+ \sim A^{1/3}$ . Also, the correction increases with transverse momentum.

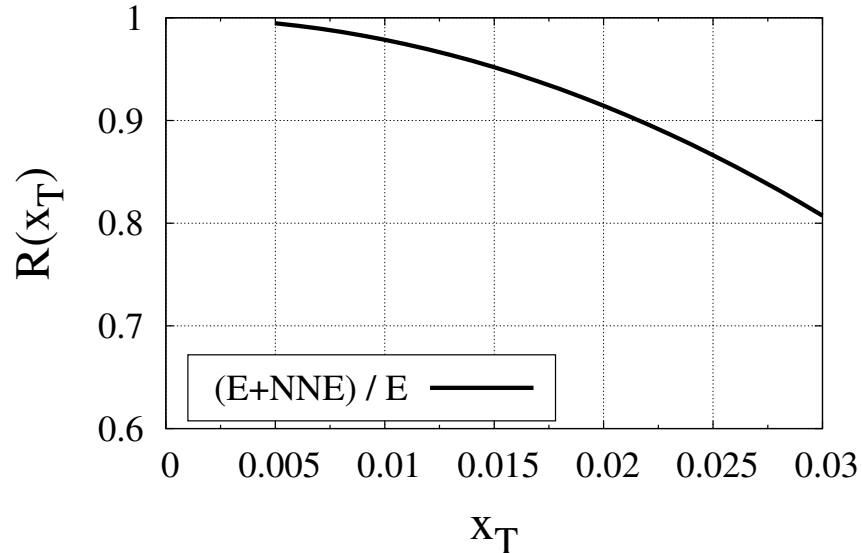


FIG. 2: Ratio of the single inclusive gluon production cross section at NNE level to that obtained in the eikonal approximation versus  $x_T = p_\perp e^{-y} / \sqrt{s}$ . See text for details.

The ratio of the gluon production cross section at NNE accuracy to the leading eikonal result is given by the square brackets in eq. (13). It is plotted in fig. 2 for a target thickness of  $\ell^+ = 7 \text{ fm} / \gamma_{\text{CM}}$  and  $p^+ = (p/\sqrt{2}) e^y$  where  $y$

denotes the rapidity of the produced gluon. We plot this ratio  $R$  versus  $x_T = p e^{-y}/\sqrt{s}$ . For  $\sqrt{s} = 200$  GeV and  $y = 0$  or  $\sqrt{s} = 5$  TeV and  $y = -3.2$ , for example,  $x_T = 0.005 - 0.03$  corresponds to transverse momenta of  $1 - 6$  GeV. The figure shows that for  $x_T \simeq 0.02$  and below the correction is reasonably small. Hence, our results justify the high-energy approximation in this regime and, furthermore, can be used to obtain more accurate estimates. On the other hand, beyond  $x_T \simeq 0.03$  the corrections grow very large and can no longer be trusted.

The NNE correction computed here represents a nuclear modification of particle production since  $\ell^+$  is proportional to the thickness of the target. The NNE suppression observed in fig. 2 therefore counteracts the nuclear Cronin enhancement due to multiple scattering[19]; see refs. [4, 13, 14] for discussions of the Cronin effect within the McLerran-Venugopalan model and refs. [15] for its evolution to small  $x$ . Detailed numerical studies of these effects are beyond the scope of this paper.

Next, we consider two gluon inclusive production. A detailed derivation is provided in appendix C. Here, we only summarize the main results.

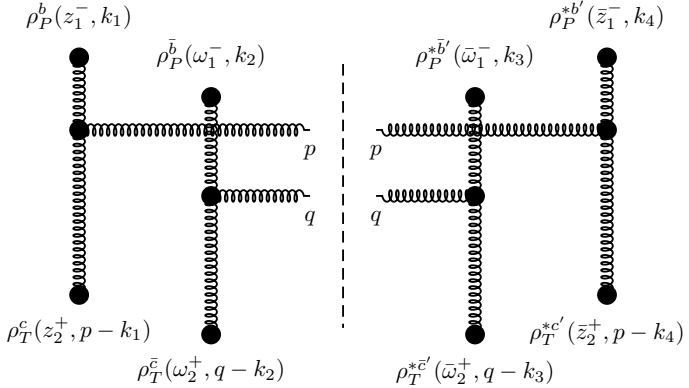


FIG. 3: Double inclusive gluon production

In the linear approximation two gluon production corresponds to the diagram shown in fig. 3 which has to be summed over all possible contractions of the sources in the projectile and target, respectively [16]. Just as in the above we assume that the projectile can be approximated by an infinitely thin shock wave but we allow for a finite thickness  $\ell^+ \sim A^{1/3}$  of the target. For simplicity, we restrict the discussion here to the local (in  $z^+$ ) model, eqs. (9,10). In this case, sub-eikonal corrections cancel when one performs a contraction of the same sources in the amplitude and in its complex conjugate (denoted as “type A” diagrams in appendix C). On the other hand, NNE corrections do not cancel when  $\rho_1$  is contracted with  $\rho_2^*$  and  $\rho_1^*$  is contracted with  $\rho_2$  (“type B” diagrams in appendix C), or when  $\rho_1$  is contracted with  $\rho_2$  and  $\rho_1^*$  with  $\rho_2^*$  (“type C” diagrams in appendix C). These diagrams again involve a correction of order

$$-\left(\frac{\ell^+ p^2}{p^+}\right)^2. \quad (15)$$

To simplify the expression here we have assumed that  $p \sim q$  while  $p^+ \ll q^+$ , i.e. that the rapidity  $y_p$  is significantly closer to that of the target beam than  $y_q$ . Note that this correction is proportional to  $A^{2/3}$ . The fact that NNE corrections do appear in the two-gluon cross section and that they are not the same for all diagrams could be important for studies of two-particle azimuthal correlations. However, more detailed computations with realistic unintegrated gluon densities, and including the dijet contribution are required [17] for more quantitative statements.

In summary, in this paper we have evaluated explicitly Wilson lines with electric field insertions to leading order in the field  $gA^-$  of the target. This determines next to eikonal (NE) and next to next to eikonal (NNE) corrections to the Lipatov vertex which are proportional to powers of the target thickness, and hence to  $A^{1/3}$ . From the vertex we have derived a  $k_T$ -factorization formula valid up to NNE accuracy. For single inclusive gluon production we find that sub-eikonal corrections cancel if a model with local (in the longitudinal coordinate  $z^+$ ) color charge correlator for the target is employed. On the other hand such corrections should be present in models with color charge correlators with finite support. Furthermore, NNE eikonal corrections also appear in correlated two gluon production, even for a local target color charge correlator. Rather than simply rescaling the two-gluon cross section we find that NNE corrections depend on the type of contractions of the sources in the target. Thus, such corrections may affect two-particle angular correlations when  $\ell^+ p^2/p^+$  is not very small.

### Acknowledgments

T.A. expresses his gratitude to the Department of Natural Sciences of Baruch College for their warm hospitality during a visit when this work was done. T.A. acknowledges support by the People Programme (Marie Curie Actions) of the European Union's Seventh Framework Programme FP7/2007-2013/ under REA grant agreement #318921; the European Research Council grant HotLHC ERC-2011-StG-279579, Ministerio de Ciencia e Innovación of Spain under project FPA2014-58293-C2-1-P, Xunta de Galicia (Consellería de Educación and Consellería de Innovación e Industria - Programa Incite), the Spanish Consolider-Ingenio 2010 Programme CPAN and FEDER. A.D. gratefully acknowledges support by the DOE Office of Nuclear Physics through Grant No. DE-FG02-09ER41620; and from The City University of New York through the PSC-CUNY Research grants 67119-0045 and 69362-0047.

### Appendix A: The Lipatov vertex to NNE level

In this appendix we provide details of the calculation of NE and NNE corrections to the Lipatov vertex. The gluon-nucleus reduced amplitude[20] at NNE accuracy [10] is given by

$$\begin{aligned} \overline{M}_\lambda^{ab}(\underline{p}, k) = & i\varepsilon_\lambda^{*i} \int d^2x e^{ix \cdot (k-p)} \left\{ 2C^i(p, k) \mathcal{U}(\ell^+, 0; x) + \frac{\ell^+}{p^+} \left[ \left( \delta^{ij} - 2p^j \frac{k^i}{k^2} \right) \mathcal{U}_{[0,1]}^j(\ell^+, 0; x) - i \frac{k^i}{k^2} \mathcal{U}_{[1,0]}(\ell^+, 0; x) \right] \right. \\ & + \left( \frac{\ell^+}{p^+} \right)^2 \left[ - \frac{k^i}{k^2} p^j p^l \mathcal{U}_{[0,2]}^{jl}(\ell^+, 0; x) - i \frac{k^i}{k^2} p^j \mathcal{U}_{[1,1]}^j(\ell^+, 0; x) + \frac{1}{2} \frac{k^i}{k^2} \mathcal{U}_{[2,0]}(\ell^+, 0; x) \right. \\ & \left. \left. + \frac{i}{4} (p^2 \delta^{ij} - 2p^i p^j) \mathcal{U}_{(A)}^j(\ell^+, 0; x) + \frac{1}{4} p^j \mathcal{U}_{(B)}^{ij}(\ell^+, 0; x) + \frac{i}{4} \mathcal{U}_{(C)}^i(\ell^+, 0; x) \right] \right\}, \end{aligned} \quad (\text{A1})$$

where  $(\underline{p}) \equiv (p^+, p)$ [21]. This expression is valid to all orders in the field of the target. To compute the Lipatov vertex we expand the standard or decorated Wilson lines to linear order in the charge density of the target,  $g\rho_T$ . For the standard Wilson line,

$$\int d^2x e^{ix \cdot (k-p)} \mathcal{U}(\ell^+, 0; x)^{ab} = (2\pi)^2 \delta(k-p) 1^{ab} + i g^2 T_c^{ab} \frac{1}{(p-k)^2} \int_0^{\ell^+} dz^+ \rho_T^c(z^+, p-k) + O(\rho_T^2). \quad (\text{A2})$$

The decorated Wilson lines that appear at NE and NNE level are Wilson lines with one or more background field insertions along the longitudinal axis from 0 to  $\ell^+$ . For the explicit expressions of these decorated Wilson lines, we refer to ref. [10]. The expansion of each field insertion starts at linear order in  $\rho_T$ . Thus, terms with multiple field insertions contribute at higher orders in  $\rho_T$  and can be neglected at linear order. Keeping this in mind, we obtain the following expressions for the decorated Wilson lines:

$$\int d^2x e^{ix \cdot (k-p)} \mathcal{U}_{[0,1]}^j(\ell^+, 0, x)^{ab} = -g^2 T_c^{ab} \frac{(p-k)^j}{(p-k)^2} \int_0^{\ell^+} dz^+ \left( \frac{z^+}{\ell^+} \right) \rho_T^c(z^+, p-k) + O(\rho_T^2) \quad (\text{A3})$$

$$\int d^2x e^{ix \cdot (k-p)} \mathcal{U}_{[1,0]}(\ell^+, 0, x)^{ab} = -ig^2 T_c^{ab} \int_0^{\ell^+} dz^+ \left( \frac{z^+}{\ell^+} \right) \rho_T^c(z^+, p-k) + O(\rho_T^2) \quad (\text{A4})$$

$$\int d^2x e^{ix \cdot (k-p)} \mathcal{U}_{[0,2]}^{jl}(\ell^+, 0, x)^{ab} = -ig^2 T_c^{ab} \frac{(p-k)^j (p-k)^l}{(p-k)^2} \int_0^{\ell^+} dz^+ \left( \frac{z^+}{\ell^+} \right)^2 \rho_T^c(z^+, p-k) + O(\rho_T^2) \quad (\text{A5})$$

$$\int d^2x e^{ix \cdot (k-p)} \mathcal{U}_{[1,1]}^j(\ell^+, 0, x)^{ab} = g^2 T_c^{ab} (p-k)^j \int_0^{\ell^+} dz^+ \left( \frac{z^+}{\ell^+} \right)^2 \rho_T^c(z^+, p-k) + O(\rho_T^2) \quad (\text{A6})$$

$$\int d^2x e^{ix \cdot (k-p)} \mathcal{U}_{[2,0]}(\ell^+, 0, x)^{ab} = ig^2 T_c^{ab}(p-k)^2 \frac{1}{2} \int_0^{\ell^+} dz^+ \left( \frac{z^+}{\ell^+} \right)^2 \rho_T^c(z^+, p-k) + O(\rho_T^2) \quad (\text{A7})$$

$$\int d^2x e^{ix \cdot (k-p)} \mathcal{U}_{(\text{A})}^j(\ell^+, 0, x)^{ab} = -g^2 T_c^{ab} \frac{(p-k)^j}{(p-k)^2} \int_0^{\ell^+} dz^+ \left( \frac{z^+}{\ell^+} \right)^2 \rho_T^c(z^+, p-k) + O(\rho_T^2) \quad (\text{A8})$$

$$\begin{aligned} \int d^2x e^{ix \cdot (k-p)} \mathcal{U}_{(\text{B})}^{ij}(\ell^+, 0, x)^{ab} &= -ig^2 T_c^{ab} [\delta^{ij} \delta^{lm} + \delta^{il} \delta^{jm} + \delta^{im} \delta^{jl}] \frac{(p-k)^l (p-k)^m}{(p-k)^2} \\ &\times \int_0^{\ell^+} dz^+ \left( \frac{z^+}{\ell^+} \right)^2 \rho_T^c(z^+, p-k) + O(\rho_T^2) \end{aligned} \quad (\text{A9})$$

$$\int d^2x e^{ix \cdot (k-p)} \mathcal{U}_{(\text{C})}^i(\ell^+, 0, x)^{ab} = g^2 T_c^{ab} (p-k)^i \int_0^{\ell^+} dz^+ \left( \frac{z^+}{\ell^+} \right)^2 \rho_T^c(z^+, p-k) + O(\rho_T^2) \quad (\text{A10})$$

Using the expressions above, it is straightforward to obtain the amplitude at order  $\rho_T$  as

$$\overline{M}_\lambda^{ab}(\underline{p}, k) = i\varepsilon_\lambda^{*i} (ig^2) T_c^{ab} \frac{1}{(p-k)^2} \int_0^{\ell^+} dz^+ 2C^i(p, k) \left\{ 1 + \frac{i}{2} p^2 \frac{z^+}{p^+} - \frac{1}{8} \left( p^2 \frac{z^+}{p^+} \right)^2 \right\} \rho_T^c(z^+, p-k) . \quad (\text{A11})$$

One can now read off the Lipatov vertex at NNE accuracy as written in eq. (6). The first term in the curly brackets corresponds to a straight line trajectory. The second and third terms account for corrections, at  $\mathcal{O}(\ell^+)$  and  $\mathcal{O}(\ell^{+2})$ , respectively, due to quantum diffusion from that classical path. The structure of the vertex in eq. (A11) suggests that the corrections to the amplitude due to a finite target thickness may exponentiate to a phase,

$$\left\{ 1 + \frac{i}{2} p^2 \frac{z^+}{p^+} - \frac{1}{8} \left( p^2 \frac{z^+}{p^+} \right)^2 \right\} \rightarrow \exp \left( \frac{i}{2} p^2 \frac{z^+}{p^+} \right) . \quad (\text{A12})$$

However, a strict proof of exponentiation would require a generalization of eq. (A1) to all orders in  $\ell^+/p^+$ .

## Appendix B: Single inclusive gluon production at NNE accuracy

The single inclusive gluon production cross section is given by

$$\begin{aligned} f^{abc} f^{ab'c'} g^6 \int \frac{d^2 k_1}{(2\pi)^2} \frac{d^2 k_2}{(2\pi)^2} \int dz_1^- dz_2^+ d\bar{z}_1^- d\bar{z}_2^+ \frac{L_i(p, k_1) L_i^*(p, k_2)}{k_1^2 k_2^2 (p-k_1)^2 (p-k_2)^2} \\ \times \left\langle \rho^b(z_1^-, k_1) \rho^{*b'}(\bar{z}_1^-, k_2) \right\rangle_P \left\langle \rho^c(z_2^+, p-k_1) \rho^{*c'}(\bar{z}_2^+, p-k_2) \right\rangle_T . \end{aligned} \quad (\text{B1})$$

With the (re-exponentiated) Lipatov vertex from above and the color charge correlator from eq. (12) this becomes

$$4N_c(N_c^2 - 1) g^4 S_\perp \int \frac{d^2 k}{(2\pi)^2} \frac{g^2 \int dz_1^- \mu_P^2}{k^2} \frac{k^2}{(p-k)^4} \ell^+ \mu_T^2 C^i(p, k) C^i(p, k) \frac{1}{\ell^{+2}} \int dz_2^+ d\bar{z}_2^+ e^{ip^2(z_2^+ - \bar{z}_2^+)/2p^+} \quad (\text{B2})$$

$$= 4N_c(N_c^2 - 1) g^2 \frac{S_\perp}{p^2} \left( \frac{4p^+}{p^2 \ell^+} \right)^2 \sin^2 \left( \frac{p^2 \ell^+}{4p^+} \right) \int \frac{d^2 k}{(2\pi)^2} \Phi_P(k^2) \frac{g^2 \ell^+ \mu_T^2}{(p-k)^2} . \quad (\text{B3})$$

Substituting the unintegrated gluon distribution of the target introduced in eq. (14) and expanding to second order in  $\ell^+$  finally leads to

$$4N_c(N_c^2 - 1) g^2 \frac{S_\perp}{p^2} \left[ 1 - \frac{1}{3} \left( \frac{p^2 \ell^+}{4p^+} \right)^2 \right] \int \frac{d^2 k}{(2\pi)^2} \Phi_P(k^2) \Phi_T((p-k)^2) . \quad (\text{B4})$$

### Appendix C: Double inclusive gluon production at NNE accuracy

The double inclusive gluon production cross section is given by

$$p^+ q^+ \frac{d\sigma}{dp^+ d^2 p dq^+ d^2 q} = f^{abc} f^{\bar{a}\bar{b}\bar{c}} f^{\bar{a}\bar{b}'\bar{c}'} f^{ab'c'} g^{12} \int \frac{d^2 k_1}{(2\pi)^2} \frac{d^2 k_2}{(2\pi)^2} \frac{d^2 k_3}{(2\pi)^2} \int dz_1^- d\bar{z}_1^- d\omega_1^- d\bar{\omega}_1^- dz_2^+ d\bar{z}_2^+ d\omega_2^+ d\bar{\omega}_2^+ \\ \times \frac{L^i(p, k_1; z_2^+)}{k_1^2(p - k_1)^2} \frac{L^{*i}(p, k_4; \bar{z}_2^+)}{k_4^2(p - k_4)^2} \frac{L^j(q, k_2; \omega_2^+)}{k_2^2(q - k_2)^2} \frac{L^{*j}(q, k_3; \bar{\omega}_2^+)}{k_3^2(q - k_3)^2} \left\langle \rho^b(z_1^-, k_1) \rho^{\bar{b}'}(\omega_1^-, k_2) \rho^{*b'}(\bar{\omega}_1^-, k_3) \rho^{*b'}(\bar{z}_1^+, k_4) \right\rangle_P \\ \times \left\langle \rho^c(z_2^+, p - k_1) \rho^{\bar{c}'}(\omega_2^+, q - k_2) \rho^{*c'}(\bar{\omega}_2^+, q - k_3) \rho^{*c'}(\bar{z}_2^+, p - k_4) \right\rangle_T \quad (C1)$$

We consider two different cases for the correlations of the color charges of the target. First, we assume that the correlator of two color charges of the target are local in longitudinal direction and use eq. (10) to compute the double inclusive gluon production cross section. Then, we consider a non-local averaging for the color charges of the target and adopt eq. (12) in the calculation of the cross section.

#### 1. Target color charge correlators with local longitudinal component

Type A contributions correspond to the following contraction on the target side.

$$\left\langle \rho^c(z_2^+, p - k_1) \rho^{\bar{c}'}(\omega_2^+, q - k_2) \rho^{*c'}(\bar{\omega}_2^+, q - k_3) \rho^{*c'}(\bar{z}_2^+, p - k_4) \right\rangle_T \rightarrow \left\langle \rho^c(z_2^+, p - k_1) \rho^{*c'}(\bar{z}_2^+, p - k_4) \right\rangle_T \\ \times \left\langle \rho^{\bar{c}'}(\omega_2^+, q - k_2) \rho^{*c'}(\bar{\omega}_2^+, q - k_3) \right\rangle_T. \quad (C2)$$

Using eq. (10) it is straightforward to see that Type A contributions to the cross section are proportional to

$$(2\pi)^4 \delta^{cc'} \delta^{\bar{c}\bar{c}'} \delta(z_2^+ - \bar{z}_2^+) \delta(\omega_2^+ - \bar{\omega}_2^+) \delta^{(2)}(k_1 - k_4) \delta^{(2)}(k_2 - k_3) \mu_T^2(z_2^+) \mu_T^2(\omega_2^+). \quad (C3)$$

However, realizing the  $\delta$ -functions in eq. (C3), one can easily see that sub-eikonal corrections to the Type A contributions for the double inclusive gluon production cross section vanish.

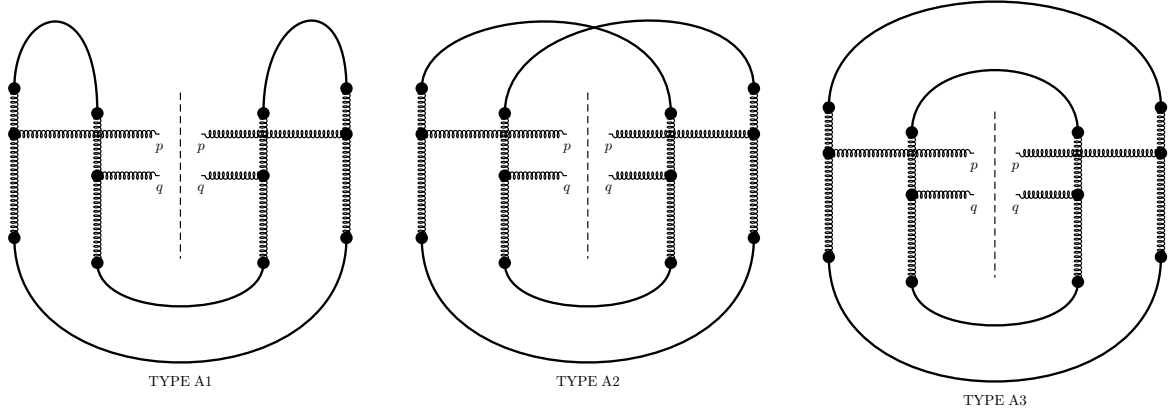


FIG. 4: Type A contributions to the double inclusive gluon production

After performing the color contractions on the projectile side we get three types of diagrams: Type A1, Type A2 and Type A3 (see Fig. 4). Each diagram has different  $\delta$ -function structure.

$$\text{Type A1} \propto (2\pi)^2 \delta^{b\bar{b}} \delta^{\bar{b}'b'} \delta(z_1^- - \omega_1^-) \delta(\bar{z}_1^- - \bar{\omega}_1^-) \delta^{(2)}(k_1 + k_2) \delta^{(2)}(k_3 + k_4) \mu_P^2(z_1^-) \mu_P^2(\bar{z}_1^-) \quad (C4)$$

$$\text{Type A2} \propto (2\pi)^2 \delta^{b\bar{b}'} \delta^{\bar{b}b'} \delta(z_1^- - \bar{\omega}_1^-) \delta(\bar{z}_1^- - \omega_1^-) \delta^{(2)}(k_1 - k_3) \delta^{(2)}(k_2 - k_4) \mu_P^2(z_1^-) \mu_P^2(\bar{z}_1^-) \quad (C5)$$

$$\text{Type A3} \propto (2\pi)^2 \delta^{b\bar{b}'} \delta^{\bar{b}b'} \delta(z_1^- - \bar{z}_1^+) \delta(\omega_1^- - \bar{\omega}_1^-) \delta^{(2)}(k_1 - k_4) \delta^{(2)}(k_2 - k_3) \mu_P^2(z_1^-) \mu_P^2(\bar{\omega}_1^-). \quad (C6)$$

Using eqs. (C3 - C6), Type A contributions to the double inclusive gluon cross section reads

$$\text{Type A1} = f^{abc} f^{\bar{a}b\bar{c}} f^{\bar{a}\bar{b}\bar{c}} f^{a\bar{b}c} S_{\perp} g^8 \int \frac{d^2 k_1}{(2\pi)^2} \frac{d^2 k_3}{(2\pi)^2} \delta^{(2)}(k_1 + k_3) \Phi_P(k_1^2) \Phi_P(k_3^2) \int dz_2^+ d\omega_2^+ \mu_T^2(z_2^+) \mu_T^2(\omega_2^+) \\ 2^4 C^i(p, k_1) C^i(p, -k_3) C^j(q, -k_1) C^j(q, k_3) \frac{k_1^2 k_3^2}{(p - k_1)^2 (p + k_3)^2 (q + k_1)^2 (q - k_3)^2} \quad (\text{C7})$$

$$\text{Type A2} = f^{abc} f^{\bar{a}b\bar{c}} f^{\bar{a}\bar{b}\bar{c}} f^{a\bar{b}c} S_{\perp} g^8 \int \frac{d^2 k_1}{(2\pi)^2} \frac{d^2 k_2}{(2\pi)^2} \delta^{(2)}(k_1 - k_2) \Phi_P(k_1^2) \Phi_P(k_2^2) \int dz_2^+ d\omega_2^+ \mu_T^2(z_2^+) \mu_T^2(\omega_2^+) \\ 2^4 C^i(p, k_1) C^i(p, k_1) C^j(q, k_2) C^j(q, k_2) \frac{k_1^2 k_2^2}{(p - k_1)^4 (q - k_2)^4} \quad (\text{C8})$$

$$\text{Type A3} = f^{abc} f^{\bar{a}b\bar{c}} f^{\bar{a}\bar{b}\bar{c}} f^{a\bar{b}c} S_{\perp}^2 g^8 \int \frac{d^2 k_1}{(2\pi)^2} \frac{d^2 k_2}{(2\pi)^2} \Phi_P(k_1^2) \Phi_P(k_2^2) \int dz_2^+ d\omega_2^+ \mu_T^2(z_2^+) \mu_T^2(\omega_2^+) \\ 2^4 C^i(p, k_1) C^i(p, k_1) C^j(q, k_2) C^j(q, k_2) \frac{k_1^2 k_2^2}{(p - k_1)^4 (q - k_2)^4} \quad (\text{C9})$$

Note that we have used eq. (14) to define the unintegrated gluon distribution of the projectile and eq. (6) for the definition of the Lipatov vertex at NNE accuracy. We would like to emphasize one more time that the sub-eikonal corrections vanish for Type A contributions and we recover the well known eikonal limit.

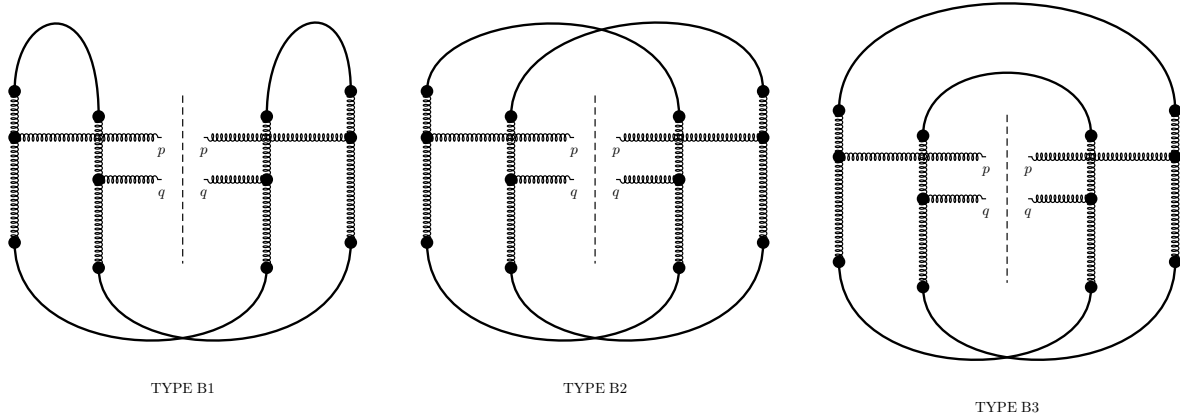


FIG. 5: Type B contributions to the double inclusive gluon production

Type B contributions correspond to the following color contraction on the target side.

$$\left\langle \rho^c(z_2^+, p - k_1) \rho^{\bar{c}}(\omega_2^+, q - k_2) \rho^{*\bar{c}'}(\bar{\omega}_2^+, q - k_3) \rho^{*c'}(\bar{z}_2^+, p - k_4) \right\rangle_T \rightarrow \left\langle \rho^c(z_2^+, p - k_1) \rho^{*\bar{c}'}(\bar{\omega}_2^+, q - k_3) \right\rangle_T \\ \times \left\langle \rho^{\bar{c}}(\omega_2^+, q - k_2) \rho^{*c'}(\bar{z}_2^+, p - k_4) \right\rangle_T. \quad (\text{C10})$$

Again, by using eq. (10), one can realize that Type B contributions are proportional to

$$(2\pi)^4 \delta^{c\bar{c}'} \delta^{\bar{c}c'} \delta(z_2^+ - \bar{\omega}_2^+) \delta(\omega_2^+ - \bar{z}_2^+) \delta^{(2)}(p - q + k_3 - k_1) \delta^{(2)}(q - p + k_4 - k_2) \mu_T^2(z_2^+) \mu_T^2(\omega_2^+). \quad (\text{C11})$$

The color contractions on the projectile side are the same as Type A diagrams. Hence, one can immediately write

the Type B contributions to the double inclusive gluon production cross section as

$$\text{Type B1} = f^{abc} f^{\bar{a}\bar{b}\bar{c}} f^{\bar{a}\bar{b}\bar{c}} f^{ab\bar{c}} S_{\perp} g^8 \int \frac{d^2 k_1}{(2\pi)^2} \frac{d^2 k_3}{(2\pi)^2} \delta^{(2)}(p - q - k_1 + k_3) \Phi_P(k_1^2) \Phi_P(k_3^2) \int dz_2^+ d\bar{z}_2^+ \mu_T^2(z_2^+) \mu_T^2(\bar{z}_2^+) 2^4 C^i(p, k_1) C^i(p, -k_3) C^j(q, -k_1) C^j(q, k_3) \frac{k_1^2 k_3^2}{(p - k_1)^2 (p + k_3)^2 (q + k_1)^2 (q - k_3)^2} \left\{ 1 - \frac{1}{8} \left( \frac{p^2}{p^+} - \frac{q^2}{q^+} \right)^2 (z_2^+ - \bar{z}_2^+)^2 \right\} \quad (C12)$$

$$\text{Type B2} = f^{abc} f^{\bar{a}\bar{b}\bar{c}} f^{\bar{a}\bar{b}\bar{c}} f^{a\bar{b}\bar{c}} S_{\perp} g^8 \delta^{(2)}(p - q) \int \frac{d^2 k_1}{(2\pi)^2} \frac{d^2 k_2}{(2\pi)^2} \Phi_P(k_1^2) \Phi_P(k_2^2) \int dz_2^+ d\bar{z}_2^+ \mu_T^2(z_2^+) \mu_T^2(\bar{z}_2^+) 2^4 C^i(p, k_1) C^i(p, k_2) C^j(q, k_1) C^j(q, k_2) \frac{k_1^2 k_2^2}{(p - k_1)^2 (p - k_2)^2 (q - k_1)^2 (q - k_2)^2} \left\{ 1 - \frac{1}{8} \left( \frac{p^2}{p^+} - \frac{q^2}{q^+} \right)^2 (z_2^+ - \bar{z}_2^+)^2 \right\} \quad (C13)$$

$$\text{Type B3} = f^{abc} f^{\bar{a}\bar{b}\bar{c}} f^{\bar{a}\bar{b}\bar{c}} f^{ab\bar{c}} S_{\perp} g^8 \int \frac{d^2 k_1}{(2\pi)^2} \frac{d^2 k_2}{(2\pi)^2} \delta^{(2)}(p - q - k_1 + k_2) \Phi_P(k_1^2) \Phi_P(k_2^2) \int dz_2^+ d\bar{z}_2^+ \mu_T^2(z_2^+) \mu_T^2(\bar{z}_2^+) 2^4 C^i(p, k_1) C^i(p, k_1) C^j(q, k_2) C^j(q, k_2) \frac{k_1^2 k_2^2}{(p - k_1)^4 (q - k_2)^4} \left\{ 1 - \frac{1}{8} \left( \frac{p^2}{p^+} - \frac{q^2}{q^+} \right)^2 (z_2^+ - \bar{z}_2^+)^2 \right\} \quad (C14)$$

Note that for the Type B contributions, next to eikonal contributions to the cross section vanish due to integration over  $z_2^+$  and  $\bar{z}_2^+$ . However, the next to next to eikonal corrections to the cross sections do not vanish.

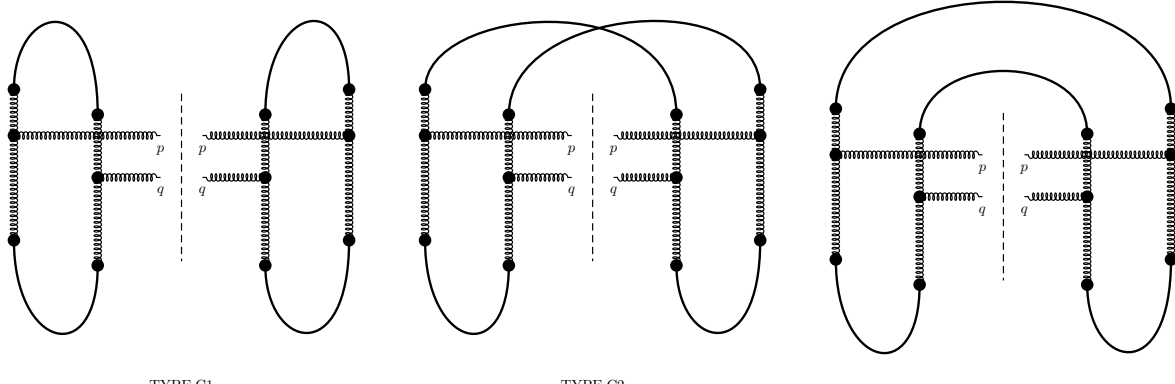


FIG. 6: Type C contributions to the double inclusive gluon production

The color contractions on the target side for Type C contributions is given by

$$\left\langle \rho^c(z_2^+, p - k_1) \rho^{\bar{c}}(\omega_2^+, q - k_2) \rho^{*\bar{c}'}(\bar{\omega}_2^+, q - k_3) \rho^{*c'}(\bar{z}_2^+, p - k_4) \right\rangle_T \rightarrow \left\langle \rho^c(z_2^+, p - k_1) \rho^{*\bar{c}}(\omega_2^+, q - k_2) \right\rangle_T \times \left\langle \rho^{\bar{c}'}(\bar{\omega}_2^+, q - k_3) \rho^{*c'}(\bar{z}_2^+, p - k_4) \right\rangle_T. \quad (C15)$$

Thus, they are proportional to

$$(2\pi)^4 \delta^{c\bar{c}} \delta^{\bar{c}'c'} \delta(z_2^+ - \omega_2^+) \delta(\bar{z}_2^+ - \bar{\omega}_2^+) \delta^{(2)}(p + q - k_1 - k_2) \delta^{(2)}(p + q - k_3 - k_4) \mu_T^2(z_2^+) \mu_T^2(\bar{z}_2^+). \quad (C16)$$

Since the color contractions on the projectile side are the same as Type A and Type B diagrams, one can write the Type C contributions to the double inclusive gluon production cross section as follows.

$$\text{Type C1} = f^{abc} f^{\bar{a}\bar{b}\bar{c}} f^{\bar{a}\bar{b}\bar{c}} f^{a\bar{b}\bar{c}} S_{\perp} g^8 \delta^{(2)}(p+q) \int \frac{d^2 k_1}{(2\pi)^2} \frac{d^2 k_3}{(2\pi)^2} \Phi_P(k_1^2) \Phi_P(k_3^2) \int dz_2^+ d\bar{z}_2^+ \mu_T^2(z_2^+) \mu_T^2(\bar{z}_2^+) 2^4 C^i(p, k_1) C^i(p, -k_3) C^j(q, -k_1) C^j(q, k_3) \frac{k_2^2 k_3^2}{(p-k_1)^2 (p+k_3)^2 (q+k_1)^2 (q-k_3)^2} \left\{ 1 - \frac{1}{8} \left( \frac{p^2}{p^+} + \frac{q^2}{q^+} \right)^2 (z_2^+ - \bar{z}_2^+)^2 \right\} \quad (C17)$$

$$\text{Type C2} = f^{abc} f^{\bar{a}\bar{b}\bar{c}} f^{\bar{a}\bar{b}\bar{c}} f^{a\bar{b}\bar{c}} S_{\perp} g^8 \int \frac{d^2 k_1}{(2\pi)^2} \frac{d^2 k_2}{(2\pi)^2} \delta^{(2)}(p+q-k_1-k_2) \Phi_P(k_1^2) \Phi_P(k_2^2) \int dz_2^+ d\bar{z}_2^+ \mu_T^2(z_2^+) \mu_T^2(\bar{z}_2^+) 2^4 C^i(p, k_1) C^i(p, k_2) C^j(q, k_1) C^j(q, k_2) \frac{k_1^2 k_2^2}{(p-k_1)^2 (p-k_2)^2 (q-k_1)^2 (q-k_2)^2} \left\{ 1 - \frac{1}{8} \left( \frac{p^2}{p^+} + \frac{q^2}{q^+} \right)^2 (z_2^+ - \bar{z}_2^+)^2 \right\} \quad (C18)$$

$$\text{Type C3} = f^{abc} f^{\bar{a}\bar{b}\bar{c}} f^{\bar{a}\bar{b}\bar{c}} f^{a\bar{b}\bar{c}} S_{\perp} g^8 \int \frac{d^2 k_1}{(2\pi)^2} \frac{d^2 k_2}{(2\pi)^2} \delta^{(2)}(p+q-k_1-k_2) \Phi_P(k_1^2) \Phi_P(k_2^2) \int dz_2^+ d\bar{z}_2^+ \mu_T^2(z_2^+) \mu_T^2(\bar{z}_2^+) 2^4 C^i(p, k_1) C^i(p, k_1) C^j(q, k_2) C^j(q, k_2) \frac{k_1^2 k_2^2}{(p-k_1)^4 (q-k_2)^4} \left\{ 1 - \frac{1}{8} \left( \frac{p^2}{p^+} + \frac{q^2}{q^+} \right)^2 (z_2^+ - \bar{z}_2^+)^2 \right\} \quad (C19)$$

## 2. Target color charge correlators with non-local longitudinal component

Using eq. (12), Type A contributions to the cross section is proportional to

$$(2\pi)^4 \delta^{cc'} \delta^{\bar{c}\bar{c}'} \delta^{(2)}(k_1 - k_4) \delta^{(2)}(k_2 - k_3) \mu_T^2 \frac{\theta[l^+ - (z_2^+ - \bar{z}_2^+)]}{l^+} \mu_T^2 \frac{\theta[l^+ - (\omega_2^+ - \bar{\omega}_2^+)]}{l^+}. \quad (C20)$$

Then, Type A1 contribution can be written as

$$\text{Type A1} = f^{abc} f^{\bar{a}\bar{b}\bar{c}} f^{\bar{a}\bar{b}\bar{c}} f^{a\bar{b}\bar{c}} S_{\perp} g^8 \int \frac{d^2 k_1}{(2\pi)^2} \frac{d^2 k_3}{(2\pi)^2} \delta^{(2)}(k_1 + k_3) \Phi_P(k_1) \Phi_P(k_3) 2^4 C^i(p, k_1) C^i(p, -k_3) C^j(q, -k_1) C^j(q, k_3) \frac{k_2^2 k_3^2}{(p-k_1)^2 (p+k_3)^2 (q+k_1)^2 (q-k_3)^2} \int_0^{l^+} dz_2^+ d\bar{z}_2^+ d\omega_2^+ d\bar{\omega}_2^+ \mu_T^2 \mu_T^2 \left[ 1 + \frac{i}{2} \frac{p^2}{p^+} (z_2^+ - \bar{z}_2^+) - \frac{1}{8} \left( \frac{p^2}{p^+} \right)^2 (z_2^+ - \bar{z}_2^+)^2 \right] \left[ 1 + \frac{i}{2} \frac{q^2}{q^+} (\omega_2^+ - \bar{\omega}_2^+) - \frac{1}{8} \left( \frac{q^2}{q^+} \right)^2 (\omega_2^+ - \bar{\omega}_2^+)^2 \right] \frac{\theta[l^+ - (z_2^+ - \bar{z}_2^+)]}{l^+} \frac{\theta[l^+ - (\omega_2^+ - \bar{\omega}_2^+)]}{l^+} \quad (C21)$$

Integration over the longitudinal coordinates gives

$$\text{Type A1} = f^{abc} f^{\bar{a}\bar{b}\bar{c}} f^{\bar{a}\bar{b}\bar{c}} f^{a\bar{b}\bar{c}} S_{\perp} g^8 \int \frac{d^2 k_1}{(2\pi)^2} \frac{d^2 k_3}{(2\pi)^2} \delta^{(2)}(k_1 + k_3) \Phi_P(k_1) \Phi_P(k_3) 2^4 C^i(p, k_1) C^i(p, -k_3) C^j(q, -k_1) C^j(q, k_3) \frac{k_1^2 k_3^2}{(p-k_1)^2 (p+k_3)^2 (q+k_1)^2 (q-k_3)^2} \mu_T^2 \mu_T^2 \frac{1}{(l^+)^2} \left\{ (l^+)^4 - \frac{1}{3} \left[ \left( \frac{p^2}{4p^+} \right)^2 + \left( \frac{q^2}{4q^+} \right)^2 \right] (l^+)^6 \right\} \quad (C22)$$

Finally, substituting the definition of the unintegrated gluon distribution of the target eq (14), Type A1 contribution reads

$$\text{Type A1} = f^{abc} f^{\bar{a}\bar{b}\bar{c}} f^{\bar{a}\bar{b}\bar{c}} f^{a\bar{b}\bar{c}} S_{\perp} g^4 \int \frac{d^2 k_1}{(2\pi)^2} \frac{d^2 k_3}{(2\pi)^2} \delta^{(2)}(k_1 + k_3) \Phi_P(k_1) \Phi_P(k_3) \Phi_T(p-k_1) \Phi_T(q-k_3) 2^4 C^i(p, k_1) C^i(p, -k_3) C^j(q, -k_1) C^j(q, k_3) \frac{k_1^2 k_3^2}{(p+k_3)^2 (q+k_1)^2} \left\{ 1 - \frac{1}{3} \left[ \left( \frac{p^2 l^+}{4p^+} \right)^2 + \left( \frac{q^2 l^+}{4q^+} \right)^2 \right] \right\} \quad (C23)$$

Similar calculations can be performed for the remaining contributions with the following results.

$$\text{Type A2} = f^{abc} f^{\bar{a}\bar{b}\bar{c}} f^{\bar{a}\bar{b}\bar{c}} f^{a\bar{b}c} S_{\perp} g^4 \int \frac{d^2 k_1}{(2\pi)^2} \frac{d^2 k_2}{(2\pi)^2} \delta^{(2)}(k_1 - k_2) \Phi_P(k_1) \Phi_P(k_2) \Phi_T(p - k_1) \Phi_T(q - k_2) \\ 2^4 C^i(p, k_1) C^i(p, k_1) C^j(q, k_2) C^j(q, k_2) \frac{k_1^2 k_2^2}{(p - k_1)^2 (q - k_2)^2} \left\{ 1 - \frac{1}{3} \left[ \left( \frac{p^2 l^+}{4p^+} \right)^2 + \left( \frac{q^2 l^+}{4q^+} \right)^2 \right] \right\} \quad (\text{C24})$$

$$\text{Type A3} = f^{abc} f^{\bar{a}\bar{b}\bar{c}} f^{\bar{a}\bar{b}\bar{c}} f^{a\bar{b}c} S_{\perp}^2 g^4 \int \frac{d^2 k_1}{(2\pi)^2} \frac{d^2 k_2}{(2\pi)^2} \Phi_P(k_1) \Phi_P(k_2) \Phi_T(p - k_1) \Phi_T(q - k_2) \\ 2^4 C^i(p, k_1) C^i(p, k_1) C^j(q, k_2) C^j(q, k_2) \frac{k_1^2 k_2^2}{(p - k_1)^2 (q - k_2)^2} \left\{ 1 - \frac{1}{3} \left[ \left( \frac{p^2 l^+}{4p^+} \right)^2 + \left( \frac{q^2 l^+}{4q^+} \right)^2 \right] \right\} \quad (\text{C25})$$

$$\text{Type B1} = f^{abc} f^{\bar{a}\bar{b}\bar{c}} f^{\bar{a}\bar{b}\bar{c}} f^{a\bar{b}\bar{c}} S_{\perp} g^4 \int \frac{d^2 k_1}{(2\pi)^2} \frac{d^2 k_3}{(2\pi)^2} \delta^{(2)}(p - q - k_1 + k_3) \Phi_P(k_1) \Phi_P(k_3) \Phi_T(p - k_1) \Phi_T(q - k_3) \\ 2^4 C^i(p, k_1) C^i(p, -k_3) C^j(q, -k_1) C^j(q, k_3) \frac{k_1^2 k_3^2}{(p + k_3)^2 (q + k_1)^2} \left\{ 1 - \frac{1}{3} \left[ \left( \frac{p^2 l^+}{4p^+} \right)^2 + \left( \frac{q^2 l^+}{4q^+} \right)^2 \right] \right\} \quad (\text{C26})$$

$$\text{Type B2} = f^{abc} f^{\bar{a}\bar{b}\bar{c}} f^{\bar{a}\bar{b}\bar{c}} f^{a\bar{b}\bar{c}} S_{\perp} g^4 \int \frac{d^2 k_1}{(2\pi)^2} \frac{d^2 k_2}{(2\pi)^2} \delta^{(2)}(p - q) \Phi_P(k_1) \Phi_P(k_2) \Phi_T(p - k_1) \Phi_T(q - k_2) \\ 2^4 C^i(p, k_1) C^i(p, k_2) C^j(q, k_1) C^j(q, k_2) \frac{k_1^2 k_2^2}{(q - k_1)^2 (p - k_2)^2} \left\{ 1 - \frac{1}{3} \left[ \left( \frac{p^2 l^+}{4p^+} \right)^2 + \left( \frac{q^2 l^+}{4q^+} \right)^2 \right] \right\} \quad (\text{C27})$$

$$\text{Type B3} = f^{abc} f^{\bar{a}\bar{b}\bar{c}} f^{\bar{a}\bar{b}\bar{c}} f^{a\bar{b}\bar{c}} S_{\perp} g^4 \int \frac{d^2 k_1}{(2\pi)^2} \frac{d^2 k_2}{(2\pi)^2} \delta^{(2)}(p - q + k_2 - k_1) \Phi_P(k_1) \Phi_P(k_2) \Phi_T(p - k_1) \Phi_T(q - k_2) \\ 2^4 C^i(p, k_1) C^i(p, k_1) C^j(q, k_2) C^j(q, k_2) \frac{k_1^2 k_2^2}{(p - k_1)^2 (q - k_2)^2} \left\{ 1 - \frac{1}{3} \left[ \left( \frac{p^2 l^+}{4p^+} \right)^2 + \left( \frac{q^2 l^+}{4q^+} \right)^2 \right] \right\} \quad (\text{C28})$$

$$\text{Type C1} = f^{abc} f^{\bar{a}\bar{b}\bar{c}} f^{\bar{a}\bar{b}\bar{c}} f^{a\bar{b}\bar{c}} S_{\perp} g^4 \int \frac{d^2 k_1}{(2\pi)^2} \frac{d^2 k_3}{(2\pi)^2} \delta^{(2)}(p + q) \Phi_P(k_1) \Phi_P(k_3) \Phi_T(p - k_1) \Phi_T(q - k_3) \\ 2^4 C^i(p, k_1) C^i(p, -k_3) C^j(q, -k_1) C^j(q, k_3) \frac{k_1^2 k_3^2}{(p + k_3)^2 (q + k_1)^2} \left\{ 1 - \frac{1}{3} \left[ \left( \frac{p^2 l^+}{4p^+} \right)^2 + \left( \frac{q^2 l^+}{4q^+} \right)^2 \right] \right\} \quad (\text{C29})$$

$$\text{Type C2} = f^{abc} f^{\bar{a}\bar{b}\bar{c}} f^{\bar{a}\bar{b}\bar{c}} f^{a\bar{b}\bar{c}} S_{\perp} g^4 \int \frac{d^2 k_1}{(2\pi)^2} \frac{d^2 k_2}{(2\pi)^2} \delta^{(2)}(p + q - k_1 - k_2) \Phi_P(k_1) \Phi_P(k_2) \Phi_T(p - k_1) \Phi_T(q - k_2) \\ 2^4 C^i(p, k_1) C^i(p, k_2) C^j(q, k_1) C^j(q, k_2) \frac{k_1^2 k_2^2}{(q - k_1)^2 (p - k_2)^2} \left\{ 1 - \frac{1}{3} \left[ \left( \frac{p^2 l^+}{4p^+} \right)^2 + \left( \frac{q^2 l^+}{4q^+} \right)^2 \right] \right\} \quad (\text{C30})$$

$$\text{Type C3} = f^{abc} f^{\bar{a}\bar{b}\bar{c}} f^{\bar{a}\bar{b}\bar{c}} f^{a\bar{b}\bar{c}} S_{\perp} g^4 \int \frac{d^2 k_1}{(2\pi)^2} \frac{d^2 k_2}{(2\pi)^2} \delta^{(2)}(p + q - k_1 - k_2) \Phi_P(k_1) \Phi_P(k_2) \Phi_T(p - k_1) \Phi_T(q - k_2) \\ 2^4 C^i(p, k_1) C^i(p, k_1) C^j(q, k_2) C^j(q, k_2) \frac{k_1^2 k_2^2}{(p - k_1)^2 (q - k_2)^2} \left\{ 1 - \frac{1}{3} \left[ \left( \frac{p^2 l^+}{4p^+} \right)^2 + \left( \frac{q^2 l^+}{4q^+} \right)^2 \right] \right\} \quad (\text{C31})$$

---

[1] Yu. V. Kovchegov, E. Levin: "Quantum Chromodynamics at High Energy", Cambridge Monographs, Cambridge Univ. Press (2012)

[2] A. Kovner, L. D. McLerran and H. Weigert, Phys. Rev. D **52**, 6231 (1995); Phys. Rev. D **52**, 3809 (1995).

[3] Yu. V. Kovchegov and D. H. Rischke, Phys. Rev. C **56**, 1084 (1997) [hep-ph/9704201].

[4] J. P. Blaizot, F. Gelis and R. Venugopalan, Nucl. Phys. A **743**, 13 (2004) [hep-ph/0402256].

[5] L. N. Lipatov, Sov. J. Nucl. Phys. **23**, 338 (1976) [Yad. Fiz. **23**, 642 (1976)]; E. A. Kuraev, L. N. Lipatov and V. S. Fadin, Sov. Phys. JETP **45**, 199 (1977) [Zh. Eksp. Teor. Fiz. **72**, 377 (1977)]; I. I. Balitsky and L. N. Lipatov, Sov. J. Nucl. Phys. **28**, 822 (1978) [Yad. Fiz. **28**, 1597 (1978)].

[6] A. Dumitru and L. D. McLerran, Nucl. Phys. A **700**, 492 (2002) [hep-ph/0105268].

- [7] I. Balitsky and A. Tarasov, JHEP **1510**, 017 (2015) [arXiv:1505.02151 [hep-ph]].
- [8] A. Babansky and I. Balitsky, Phys. Rev. D **67**, 054026 (2003).
- [9] T. Altinoluk, N. Armesto, G. Beuf, M. Martinez and C. A. Salgado, JHEP **1407**, 068 (2014) [arXiv:1404.2219 [hep-ph]].
- [10] T. Altinoluk, N. Armesto, G. Beuf and A. Moscoso, JHEP **1601**, 114 (2016) [arXiv:1505.01400 [hep-ph]].
- [11] L. D. McLerran and R. Venugopalan, Phys. Rev. D **49**, 2233 (1994), Phys. Rev. D **49**, 3352 (1994); Yu. V. Kovchegov, Phys. Rev. D **54**, 5463 (1996).
- [12] T. Lappi, Eur. Phys. J. C **55**, 285 (2008) [arXiv:0711.3039 [hep-ph]].
- [13] J. Jalilian-Marian, Y. Nara and R. Venugopalan, Phys. Lett. B **577**, 54 (2003) [nucl-th/0307022].
- [14] D. Kharzeev, Y. V. Kovchegov and K. Tuchin, Phys. Rev. D **68**, 094013 (2003) [hep-ph/0307037]; Phys. Lett. B **599**, 23 (2004) [hep-ph/0405045].
- [15] J. L. Albacete, N. Armesto, A. Kovner, C. A. Salgado and U. A. Wiedemann, Phys. Rev. Lett. **92**, 082001 (2004) [hep-ph/0307179];  
also, sec. VI in J. L. Albacete, A. Dumitru, H. Fujii and Y. Nara, Nucl. Phys. A **897**, 1 (2013) [arXiv:1209.2001 [hep-ph]].
- [16] A. Dumitru, F. Gelis, L. McLerran and R. Venugopalan, Nucl. Phys. A **810**, 91 (2008) [arXiv:0804.3858 [hep-ph]]; A. Dumitru, K. Dusling, F. Gelis, J. Jalilian-Marian, T. Lappi and R. Venugopalan, Phys. Lett. B **697**, 21 (2011) [arXiv:1009.5295 [hep-ph]].
- [17] The eikonal case has been studied in detail by K. Dusling and R. Venugopalan, Phys. Rev. D **87**, no. 5, 051502 (2013) [arXiv:1210.3890 [hep-ph]]; Phys. Rev. D **87**, no. 5, 054014 (2013) [arXiv:1211.3701 [hep-ph]].
- [18] The most direct way to see this is to note that the correction in curly brackets in eq. (6) corresponds to the first three terms in the Taylor series expansion of the phase  $\exp\left(\frac{i}{2}p^2\frac{z_2^+}{p^+}\right)$ .
- [19] Our result does not, of course, account for multiple scattering since we expanded the amplitude to linear order in the field of the target.
- [20] To obtain the field analogous to eq. (1) one would strip off the polarization vector, multiply by the projectile charge density  $g\rho_P(z_1^-, k)$ , and integrate over  $dz_1^-$  and  $d^2k/(2\pi)^2$ .
- [21] The expression written in ref. [10] is missing a factor of 1/2 in the term  $\sim \mathcal{U}_{[0,2]}^{jl}(\ell^+, 0; x)$  which we have corrected.